Journal of Power Sources 247 (2014) 687–691

Contents lists available at ScienceDirect

Journal of Power Sources

journal homepage: www.elsevier.com/locate/jpowsour

Short communication

Crystal orientation of epitaxial $LiCoO_2$ films grown on $SrTiO_3$ substrates

Kazunori Nishio [a], Tsuyoshi Ohnishi [a, b, c, d, *], Kosho Akatsuka [b], Kazunori Takada [a, b, c, d]

[a] Global Research Center for Environment and Energy Based on Nanomaterials Science (GREEN), National Institute for Materials Science (NIMS), 1-1 Namiki, Tsukuba, Ibaraki 305-0044, Japan
[b] NIMS-TOYOTA Materials Center of Excellence for Suitable Mobility, National Institute for Materials Science (NIMS), 1-1 Namiki, Tsukuba, Ibaraki 305-0044, Japan
[c] International Center for Materials Nanoarchitectonics (MANA), National Institute for Materials Science (NIMS), 1-1 Namiki, Tsukuba, Ibaraki 305-0044, Japan
[d] Environment and Energy Materials Division, National Institute for Materials Science (NIMS), 1-1 Namiki, Tsukuba, Ibaraki 305-0044, Japan

HIGHLIGHTS

- Crystal orientation of epitaxial $LiCoO_2$ thin films on $SrTiO_3$ substrates is revealed via X-ray pole figure measurement.
- $LiCoO_2$ thin films on $SrTiO_3$ (100) and (110) have a cube-on-cube orientation relationship with the substrates.
- $LiCoO_2$ film is predominantly (001)-oriented on (111) $SrTiO_3$, and the orientation relationship is accompanied with 60° in-plane rotation.

ARTICLE INFO

Article history:
Received 5 July 2013
Received in revised form
24 August 2013
Accepted 30 August 2013
Available online 12 September 2013

Keywords:
$LiCoO_2$
Epitaxial thin film
Pulsed laser deposition
X-ray pole figure measurement
All-solid-state battery

ABSTRACT

$LiCoO_2$ (LCO) thin films are epitaxially grown on (100), (110) and (111) 0.5 wt% Nb-doped $SrTiO_3$ (Nb:STO) substrates by pulsed laser deposition and their crystalline orientation relationship investigated via X-ray pole figure measurement. This investigation reveals that the LCO films grown on Nb:STO (100) and (110) have a cube-on-cube orientation relationship with the substrates to be (104)- and (018)-oriented, respectively, while the relationship is accompanied with 60° in-plane rotation on (111) Nb:STO to yield a predominantly (001)-oriented LCO film. The (104)-oriented LCO film on (100) Nb:STO substrate exhibits high rate capability up to 100 C.

1. Introduction

Lithium-ion batteries power most of today's portable electronics and, in enlarged form, hybrid electric vehicles. On the other hand, there is also increasing demand for micro-batteries including thin-film batteries for use in micro-devices such as MEMS and drug delivery systems. In thin-film batteries, thick electrodes are necessary to store a large amount of energy within a limited footprint. However, increased thickness usually lowers rate capability; one of the dominant rate-determining factors is grain boundary resistance. One way to overcome this problem is forming an active material layer without grain boundaries, which can be achieved through epitaxial growth of the active material into single crystal [1,2]. In addition, in the case of $LiCoO_2$ (LCO), which is a typical cathode material, crystal orientation in the epitaxial thin film will also affect the electrode performance, because LCO has a layered rock-salt structure to show anisotropic ionic conduction. An earlier study has demonstrated that the crystal orientation of epitaxial LCO thin films is controllable by depositing the films on a different lattice plane of a $SrTiO_3$ (STO) substrate [3]. In this study, we prepared epitaxial LCO thin films in line with the same approach and characterized the LCO thin films by X-ray pole figure measurement in order to clarify the epitaxial relationship.

* Corresponding author. National Institute for Materials Science (NIMS), 1-1 Namiki, Tsukuba, Ibaraki 305-0044, Japan. Tel.: +81 29 860 4366; fax: +81 29 854 9061.
E-mail address: OHNISHI.Tsuyoshi@nims.go.jp (T. Ohnishi).

0378-7753/$ – see front matter © 2013 Elsevier B.V. All rights reserved.
http://dx.doi.org/10.1016/j.jpowsour.2013.08.132

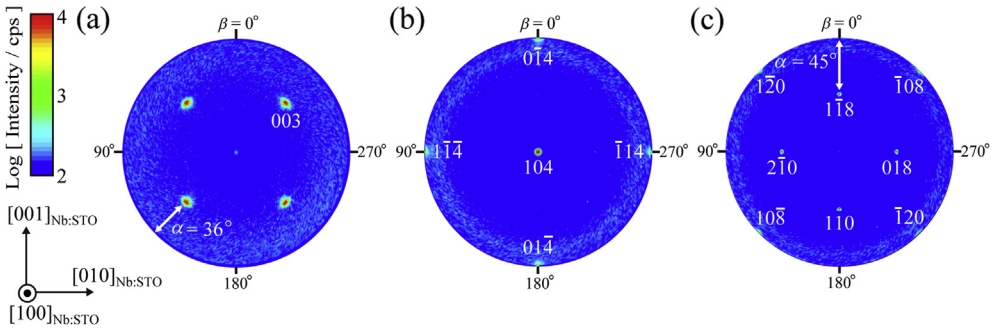

Fig. 1. X-ray pole figures for an LCO film on a Nb:STO (100) substrate. (a) 003_{LCO}, (b) 104_{LCO}, and (c) $110_{LCO}/018_{LCO}$.

2. Experimental

Epitaxial LCO thin films were grown on electron-conductive 0.5 wt% Nb-doped $SrTiO_3$ (Nb:STO) single crystal substrates with Φ10 mm × 0.5 mm^t in order to ensure current collection during electrochemical measurement. The crystal orientation of the LCO films was characterized using X-ray diffraction techniques, including pole figure measurement.

The films were deposited on (100), (110), and (111) Nb:STO substrates by pulsed laser deposition (PLD). Sintered $Li_{1.1}CoO_{2+\delta}$ pellet (TOSHIMA Manufacturing Co., Ltd.) was used as the PLD target. A KrF excimer laser (λ = 248 nm) was operated at a repetition rate of 10 Hz for the target ablation. Our recent reports on thin-film growth have revealed that ablation laser energy density (fluence) and oxygen pressure (P_{O2}) are key parameters for stoichiometric film growth [4]. In the present study, fluence and P_{O2} were fixed at 0.37 J cm^{-2} and 0.1 Pa, respectively. The substrate was heated to 500 °C during the deposition. These ablation conditions gave a growth rate of 0.039 Å s^{-1}. After deposition, the LCO film was annealed in a PLD chamber at 700 °C under P_{O2} of 10^3 Pa for 1 h to improve its crystallinity.

The crystal orientation of the LCO films was investigated by in-plane pole figure measurement [5] using an X-ray diffractometer (XRD, Rigaku, SmartLab) equipped with a rotating Cu target. The pole figures were taken for reflections of LCO 003 (denoted by 003_{LCO}, and likewise hereafter), 104_{LCO}, 110_{LCO}, and 018_{LCO} with a step of 1.0°. Prior to the pole figure measurement, asymmetric diffraction measurements were performed in addition to out-of-plane and in-plane measurements with 2-bounce Ge 220 monochromated CuKα_1 radiation in order to determine the 2θ values precisely for each reflection. Meanwhile, non-monochromated X-ray was used in the pole figure measurement to obtain high diffraction intensity. It should be noted that the 2θ values for 110_{LCO} and 018_{LCO}, both of which correspond to an after-mentioned 220 reflection from a cubic NaCl structure, are too close to differentiate under the non-monochromated X-ray. In fact, the pole figures we obtained for the 110_{LCO} and 018_{LCO} reflections are quite similar to each other. Therefore, they are presented as $110_{LCO}/018_{LCO}$ pole figures in this paper.

An all-solid-state cell was fabricated in order to investigate electrode performance. The LCO film for the electrochemical measurement was annealed additionally in air at 700 °C for 5 h after the annealing in the chamber in order to further promote crystallization. Powder $Li_{3.25}Ge_{0.25}P_{0.75}S_4$ (thio-LISICON [6]) was used as the solid electrolyte. An In–Li alloy was selected as the counter electrode and formed by attaching a piece of lithium (2 mg) to indium foil (60 mg). The surface of LCO film was coated with a Li_3PO_4 (LPO) layer before the cell assembly, otherwise the interfacial resistance between the LCO film and the solid electrolyte was too high to investigate the electrode properties. The high resistance comes from a highly-resistive space-charge layer formed at the LCO/sulfide electrolyte interface, and the formation of the resistive layer can be suppressed by interposition of an oxide solid electrolyte layer at the interface [7–9]. Also in this study, the surface of the epitaxial LCO thin film was coated with 10 nm of LPO by PLD as reported in Ref. [10], which reduces the interfacial resistance to be low enough to investigate the electrode properties. The LPO-coated LCO film on the Nb:STO substrate and the In–Li alloy were attached to both sides of a thio-LISICON layer (150 mg) as working and counter electrodes, respectively, and they were pressed together at around 500 MPa to form a three-layered pellet with a 10 mm diameter. The LCO film was then charged and discharged at room temperature using a potentiogalvanostat (VSP, Bio-Logic). Because the electrode potential of the In–Li alloy counter electrode is 0.62 V *vs.* Li^+/Li, the upper cutoff voltage was set at 3.58 V in order to charge the epitaxial LCO thin film up to 4.2 V *vs.* Li^+/Li, which corresponds to charging up to $Li_{0.5}CoO_2$ [11]. The charging rate was fixed at 0.01 C, while the discharging rate was varied from 0.01 C to 100 C, where the rate of 137 mA g^{-1} was defined as 1 C. The specific capacity was estimated based on the film thickness as determined by X-ray reflectivity measurement and the theoretical density of 5.0 g cm^{-3}.

3. Results and discussion

Fig. 1 shows the X-ray pole figures for the 60.2 nm^t LCO film on the Nb:STO (100) substrate. All the pole figures exhibit four-fold symmetry, which is consistent with the crystal symmetry of the Nb:STO (100) plane. The 003_{LCO} reflections appear as spots at α = 36° (α: angle from substrate surface) as shown in Fig. 1(a), which correspond to the <111> directions of the Nb:STO substrate and thus indicate that the LCO film consists of four types of domains with their *c*-axes parallel to the $<111>_{Nb:STO}$ directions. On the other hand, Fig. 1(b) illustrates that the pole located at α = 90° (center of pole figure, surface normal) originates from 104_{LCO} reflections, which reveals that the epitaxial LCO thin film is (104)-oriented on the Nb:STO (100) substrate as reported in a previous study [3]. All the spots in Fig. 1(b) and (c) can be indexed on the basis of a domain, which gives the 003 reflection at α = 36° and β = 315° in Fig. 1(a). As shown in Fig. 1(b), the $<104>_{LCO}$ reflections give the poles in $<100>_{Nb:STO}$ directions, indicating a crystal orientation relationship of $<104>_{LCO}||<100>_{Nb:STO}$. Instead, the positions of the $110_{LCO}/018_{LCO}$ reflections in Fig. 1(c) indicate that both $<110>_{LCO}$ and $<018>_{LCO}$ are parallel to $<110>_{Nb:STO}$. It goes without saying that the poles from the other three domains in Fig. 1(a) should give the same patterns due to their four-fold symmetry, which overlaps into the pole figures.

This epitaxial relationship is explainable by the structural similarities between LCO and STO. LCO has an NaCl-type structure, where Li and Co are ordered in the cation sites among a face-

centered-cubic (fcc) oxygen array to form alternate Li and Co layers along the [111] direction in the NaCl-type cubic lattice (hereinafter denoted by $[111]_{NaCl}$). The cation ordering elongates the cubic lattice along the $[111]_{NaCl}$ and lowers the symmetry to rhombohedral, as illustrated in Fig. 2, where the rhombohedral structure of LCO is expressed in a hexagonal cell [13]. On the other hand, STO has a cubic perovskite structure. Because the perovskite structure is very similar in oxygen arrangement to the NaCl-type structure, the LCO film grown on the STO substrate is expected to have a cube-on-cube relationship (Fig. 2). The elongation from cubic to rhombohedral makes $(1/2\ 1/2\ 1/2)_{NaCl}$ and $(200)_{NaCl}$ into $(003)_{LCO}$ and $(104)_{LCO}$, respectively, and splits $\{220\}_{NaCl}$ into $(110)_{LCO}$ and $(018)_{LCO}$. Therefore, the LCO film has the (104) orientation, because $(104)_{LCO}$ corresponding to $(200)_{NaCl}$ should be parallel to the $(100)_{STO}$ surface in the cube-on-cube epitaxy. In addition, Li and Co are ordered along the four different $<111>_{NaCl}$ directions to the same degree to give the four-domain structure.

Pole figures for the 65.6 nm^t epitaxial LCO thin film on the Nb:STO (110) substrate in Fig. 3 indicate that the cube-on-cube relationship holds for the epitaxial growth on the Nb:STO (110) substrate. Poles for the 003_{LCO} and 104_{LCO} reflections are located in the $<111>_{Nb:STO}$ and $<100>_{Nb:STO}$ directions, respectively, and poles for the 110_{LCO} and 018_{LCO} reflections are in the $<110>_{Nb:STO}$ directions, as expected from the cube-on-cube relationship. The two spots in Fig. 3(a) suggest that the film has a two-domain structure, while the film on Nb:STO (100) has a four-domain structure.

The four $<111>_{Nb:STO}$ axes in the Nb:STO (100) substrate are equivalent not only in terms of crystal structure, but also in terms of their orientation relationship with the substrate surface, and thus Li and Co are ordered along the four axes equally to give the commensurate four-domain structure. In contrast, they are not equivalent in terms of their orientation relationship with the Nb:STO (110) substrate: $[111]_{Nb:STO}$ and $[11\bar{1}]_{Nb:STO}$ make an angle of 55° with the substrate surface, while $[\bar{1}11]_{Nb:STO}$, $[1\bar{1}\bar{1}]_{Nb:STO}$, $[1\bar{1}1]_{Nb:STO}$, and $[\bar{1}1\bar{1}]_{Nb:STO}$ lie along the surface. Absence of poles at $\alpha = 0°$ indicates that the LCO film does not include domains with the *c*-axis parallel to the in-plane $<111>_{Nb:STO}$; the *c*-axis in the domains is parallel to $[111]_{Nb:STO}$ or $[11\bar{1}]_{Nb:STO}$. The poles are indexed on the basis of the domain with $[001]_{LCO}||[111]_{Nb:STO}$, which gives a pole for the 003 reflection at $\alpha = 55°$ and $\beta = 270°$. In Fig. 3(c), the Miller index for the pole at $\alpha = 90°$ is 018, which indicates that the LCO film has a (018) orientation, although it has been reported that a (110)-oriented LCO thin film has been grown on a Nb:STO (110) substrate [3]. The difference may derive from different growth conditions; however, the (018) orientation seems preferable for the reasons described below.

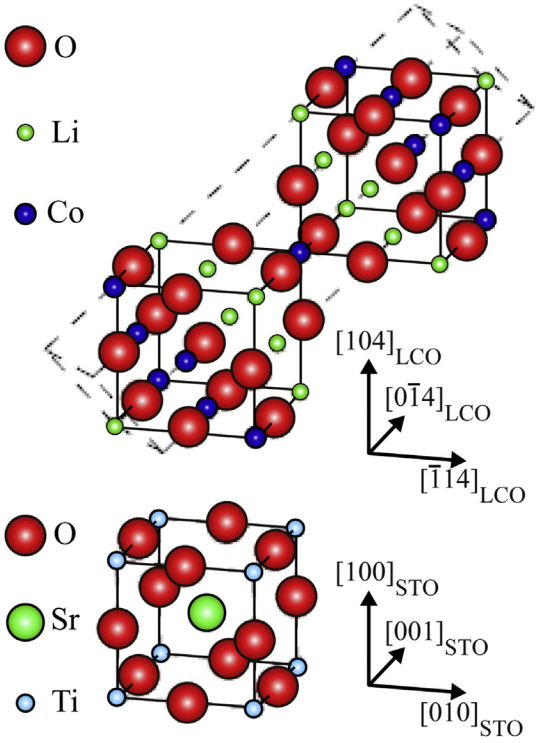

Fig. 2. Schematic representation of cube-on-cube configuration between LCO and STO. Li and Co are ordered in the NaCl-type cubic lattice indicated by the solid lines to make a hexagonal unit cell for LCO, which is indicated by dashed lines. The crystal structures were drawn by VESTA [12].

The lattice mismatch between the LCO thin film and the Nb:STO substrate is smaller in the (018) orientation than in the (110) orientation. In the (018)-oriented LCO thin film on the Nb:STO (110) substrate, $[01\bar{4}]_{LCO}$ and $[2\bar{1}0]_{LCO}$ are parallel to $[001]_{Nb:STO}$ and $[1\bar{1}0]_{Nb:STO}$, and the lattice mismatches in those directions are 2.6% and 2%, respectively. In contrast, the corresponding mismatches in $[\bar{1}14]_{LCO}$ and $[1\bar{1}8]_{LCO}$ in the (110)-oriented LCO thin film are 2.6% and 3.3%, respectively. Moreover, first principles calculations have revealed that the (001) surface has the lowest surface energy among several surfaces of LCO, while surface energy for (110) is quite high [14]. The difference in surface energy will make the (110) orientation less preferential on $(110)_{Nb:STO}$, causing the (001) orientation predominant on $(111)_{Nb:STO}$ to show a (001) surface, as described below.

Unlike the above cases, epitaxial growth on the Nb:STO (111) substrate does not conform to the simple cube-on-cube relationship. The 003 reflections from the 52.5 nm^t LCO film on the Nb:STO (111) substrate appear as four spots as shown in Fig. 4(a), which suggest the four-domain structure of the film. The intensity is higher by several orders of magnitude at $\alpha = 90°$, indicating a predominant (001) orientation with $[001]_{LCO}||[111]_{Nb:STO}$. It is expected from the cube-on-cube relationship that the other three weak spots come from domains with $[001]_{LCO}$ parallel to the other $<111>_{Nb:STO}$ directions and thus the (012) orientation. In fact, spots are located at 70° from the $[111]_{Nb:STO}$ direction, which is consistent with the angle between $[111]_{Nb:STO}$ and $[11\bar{1}]_{Nb:STO}$. However, they are not in the other $<111>_{Nb:STO}$ directions; the pole figure indicates that the three weak $[001]_{LCO}$ spots are rotated by 60° in β angle with respect to the other $<111>_{Nb:STO}$ directions.

In fact, all the other poles appear with 60° in-plane rotation from that expected based on the cube-on-cube relationship as shown in Fig. 4(b) and (c). It should be noted that pole figures for the 104_{LCO} and $110_{LCO}/018_{LCO}$ reflections have clear six spots at $\alpha = 35°$ and 55°, respectively. At a glance, those spots seem to indicate coexistence of the 60°-rotated and non-rotated domains. However, asymmetric 2θ-ω scans using CuKα_1 radiation has revealed that the poles at the non-rotated positions are attributable to $200_{Nb:STO}$ and $220_{Nb:STO}$ reflections from the substrate, respectively, generated by CuKβ radiation, because non-monochromated radiation includes a 0.5% Kβ line [5], and the $200_{Nb:STO}$ and $220_{Nb:STO}$ reflections by CuKβ coincide with 104_{LCO} and $110_{LCO}/018_{LCO}$ reflections by CuKα, respectively.

This in-plane arrangement may be explainable by the surface termination state of the Nb:STO (111) substrate. A (111)-oriented STO consists of Ti and SrO_3 layers stacked alternately in the $[111]_{STO}$ direction. Although $[111]_{STO}$ is a three-fold inversion axis, a SrO_3-terminated surface has a trigonal lattice with six-fold rotational symmetry, which should give coexistence of the 60°-rotated and non-rotated LCO domains at an equal rate. However, this is not the case, as shown in Fig. 4. In contrast, a Ti-terminated surface has three-fold symmetry. On this surface, the 60°-rotated domain

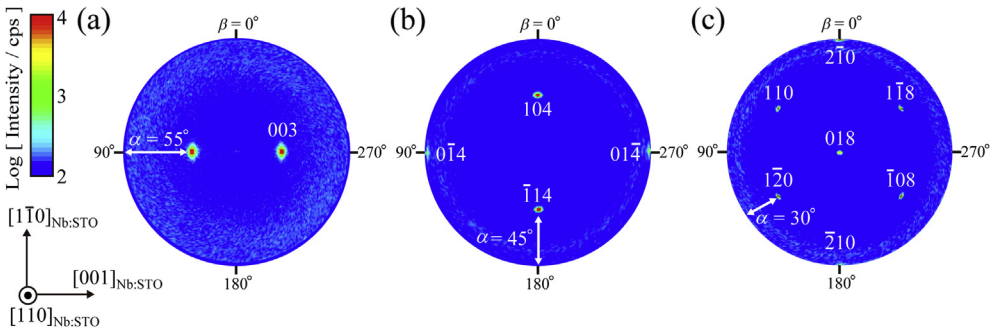

Fig. 3. X-ray pole figures for an LCO film on a Nb:STO (110) substrate. (a) 003_{LCO}, (b) 104_{LCO}, and (c) $110_{LCO}/018_{LCO}$.

seems feasible as compared to the non-rotated one, in view of the interface matching with Li/Co-terminated LCO, where the cube-on-cube configuration is broken at the interface. Such rotation often is observed at heteroepitaxial interfaces between STO (111) and Pt (111) [15,16].

Both the (001) and (012) orientations of LCO on Nb:STO (111) are conceivable due to the similarity of their oxygen arrays of LCO. However, the predominant (001) orientation of LCO was observed in this study. From the standpoint of lattice matching between LCO and Nb:STO, the (001) orientation of LCO is more favorable than the (012) orientation on the Nb:STO (111) substrate. In the (001)-oriented LCO domain on the Nb:STO (111) substrate, $[\bar{1}10]_{LCO}$ is parallel to $[10\bar{1}]_{Nb:STO}$, and the corresponding mismatch in direction is 2%. Meanwhile, in the (012)-orientated LCO domain, $[10\bar{8}]_{LCO}$ is parallel to $[10\bar{1}]_{Nb:STO}$, and the corresponding mismatch is 3.3%. Preferential orientation would stem from better lattice matching between the LCO film and the Nb:STO substrate as well as surface energy as described above in the (018)-oriented LCO thin film on the Nb:STO (110) substrate.

Additionally, six 104_{LCO} poles with intensity values close to the background level were observed at 30° rotation in β angle from the $200_{Nb:STO}$ poles, as shown in Fig. 4(b). This fact indicates the presence of two other *c*-axis-oriented domain structures that are rotated by 30° along the $[111]_{Nb:STO}$ axis. A rotational transition between the cube-on-cube configuration and 30° in-plane rotation has been found in NaCl-type MgO (111) film [17] and Wurzite AlN (0001) film [18,19] on STO (111) with dependence on film growth temperature. In the case of MgO, it has also been pointed out that the 30° rotational configuration is predominant on the SrO_3-terminated STO substrate. Although further research is needed to find the origin of the orientation relationship between the LCO thin film and the Nb:STO (111) substrate, in-plane rotational configurations of the LCO film may reflect the surface termination state of the Nb:STO (111) substrate.

Electrode properties were investigated in order to confirm that the obtained epitaxial films have characteristics of LCO in terms of electrochemistry as well as crystallography. Fig. 5 shows discharge curves for a (104)-oriented film with the thickness of 76.9 nm at various discharging rates. Capacity at a low discharge rate is not high; the discharge capacity at 0.01 C is 75 mAh g^{-1}, while ideal capacity is 137 mAh g^{-1}. Inclusion of impurities is a possible reason for the low capacity; however, Co_3O_4, which is the most conceivable impurity phase, was not detected in the Raman spectra from the films (not shown). Therefore, it can be concluded that the low value of capacity originates from overestimation of the film weight, which is calculated based on the theoretical specific weight of LCO. In spite of the low capacity at the low rate of discharge, 35% of capacity at 0.01 C is kept even at a high rate of discharge with 100 C, which indicates that epitaxial growth is a promising approach for overcoming the low rate capability from which all-solid-state systems suffer.

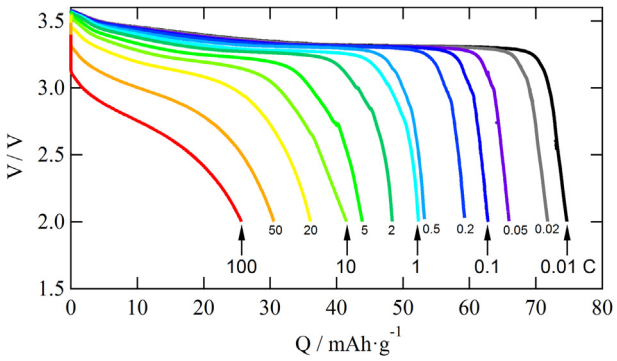

Fig. 5. Discharge curves for an all-solid-state battery using a (104)-oriented LCO epitaxial thin film on a Nb:STO (100) substrate. Discharging in the range from 0.01 C to 100 C was performed after charging at 0.01 C.

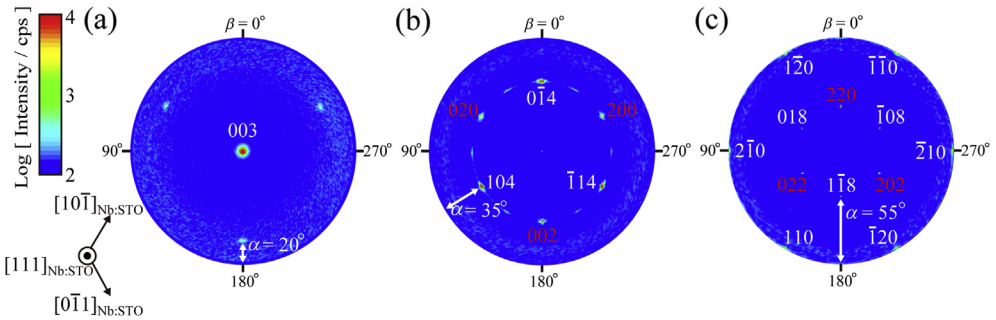

Fig. 4. X-ray pole figures for an LCO film on a Nb:STO (111) substrate. (a) 003_{LCO}, (b) 104_{LCO}, and (c) $110_{LCO}/018_{LCO}$. Poles labeled with red Miller indices in (b) and (c) are $200_{Nb:STO}$ and $220_{Nb:STO}$ reflections, respectively, by CuKβ radiation.

This paper presents discharge curves only for a (104)-oriented film, because (001) plane is the most upright on the substrate surface in the (104) orientation to facilitate access to the interlayer galleries. It is indeed interesting to examine orientation dependence of the electrode properties, and thus the same experiment has been performed for the films with different orientations. However, because not only crystal orientation but also surface morphology, for instance, affects the electrochemical reactions, it is almost impossible to discuss the orientation dependence only from the comparison between the discharge curves without unifying other parameters. Some additional electrochemical measurements and analyses are under progress in order to reveal the orientation effects, which will be reported in near future.

4. Conclusions

In summary, X-ray pole figure measurement in the present study has revealed that LCO films are epitaxially grown on single-crystal Nb:STO substrates on the basis of the cube-on-cube relationship of the oxygen arrays, where Li and Co layers are stacked alternately along the diagonals of the cube. An LCO thin film on a Nb:STO (100) substrate shows a (104) orientation and four-domain structures due to the equivalence in the diagonals. In contrast, the film on a Nb:STO (110) substrate has two (018)-oriented domains, although a (110) orientation is also possible based on the cube-on-cube epitaxy. The cube-on-cube configuration is accompanied with 60° in-plane rotation in the epitaxial growth on a Nb:STO (111) substrate. The LCO film grown on Nb:STO (111) is predominantly (001)-oriented with a minor amount of (012)-oriented domains. The rate capability of the (104)-oriented LCO thin film demonstrates that epitaxial growth is a promising way to realize high-performance all-solid-state batteries.

Acknowledgments

This work was partially supported by JSPS KAKENHI Grant Number 25420724 and MEXT Program for Development of Environmental Technology using Nanotechnology.

References

[1] T. Ohnishi, B.T. Hang, X.X. Xu, M. Osada, K. Takada, J. Mater. Res. 25 (2010) 1886–1889.
[2] M. Hirayama, K. Kim, T. Toujigamori, W. Cho, R. Kanno, Dalton Trans. 40 (2011) 2882.
[3] M. Hirayama, N. Sonoyama, T. Abe, M. Minoura, M. Ito, D. Mori, A. Yamada, R. Kanno, T. Terashima, M. Takano, K. Tamura, J. Mizuki, J. Power Sources 168 (2007) 493–500.
[4] T. Ohnishi, K. Takada, Appl. Phys. Express 5 (2012) 055502.
[5] Rigaku J. 27 (2011) 2.
[6] R. Kanno, M. Murayama, J. Electrochem. Soc. 148 (2001) A742–A746.
[7] N. Ohta, K. Takada, L. Zhang, R. Ma, M. Osada, T. Sasaki, Adv. Mater. 18 (2006) 2226–2229.
[8] N. Ohta, K. Takada, I. Sakaguchi, L. Zhang, R. Ma, K. Fukuda, M. Osada, T. Sasaki, Electrochem. Commun. 9 (2007) 1486–1490.
[9] X.X. Xu, K. Takada, K. Watanabe, I. Sakaguchi, K. Akatsuka, B.T. Hang, T. Ohnishi, T. Sasaki, Chem. Mater. 23 (2011) 3798–3804.
[10] X.X. Xu, K. Takada, K. Fukuda, T. Ohnishi, K. Akatsuka, M. Osada, B.T. Hang, K. Kumagai, T. Sekiguchi, T. Sasaki, Energy Environ. Sci. 4 (2011) 3059–3512.
[11] T. Ohzuku, A. Ueda, J. Electrochem. Soc. 141 (1994) 2972–2977.
[12] The crystal structures were drawn by using VESTA K. Momma, F. Izumi, J. Appl. Crystallogr. 44 (2011) 1272–1276.
[13] T.A. Hewston, B.L. Chamberland, J. Phys. Chem. Solids 48 (1987) 97–108.
[14] D. Kramer, G. Ceder, Chem. Mater. 21 (2009) 3799–3809.
[15] A. Asthagiri, C. Niederberger, A.J. Francis, L.M. Porter, P.A. Salvador, D.S. Sholl, Surf. Sci. 537 (2003) 134–152.
[16] S. Schmidt, D.O. Klenov, S.P. Keane, J. Lu, T.E. Mates, S. Stemmer, Appl. Phys. Lett. 88 (2006) 131914.
[17] K. Matsuzaki, H. Takagi, H. Hosono, T. Susaki, Phys. Rev. B 84 (2011) 235448.
[18] Z.Q. Yao, X. Fan, B. He, W.J. Zhang, I. Bello, S.T. Lee, X.M. Meng, Appl. Phys. Lett. 92 (2008) 241911.
[19] Z.Q. Yao, X. Fan, B. He, W.J. Zhang, I. Bello, S.T. Lee, X.M. Meng, Appl. Phys. Lett. 96 (2010) 109901.